Complex network analysis of arboviruses in the same geographic domain: Differences and similarities

Eslaine S. Santos [a,1], José G.V. Miranda [b,*,1], Hugo Saba [c,d], Lacita M. Skalinski [e,f], Marcio L.V. Araújo [g], Rafael V. Veiga [a,h], Maria da Conceição N. Costa [e], Luciana L. Cardim [a], Enny S. Paixão [a,i], Maria Glória Teixeira [a,e], Roberto F.S. Andrade [a,b,1], Maurício L. Barreto [a,e]

[a] Center of Data and Knowledge Integration for Health (CIDACS), Gonçalo Moniz Institute, Oswaldo Cruz Foundation, Salvador, Bahia, Brazil
[b] Physics Institute, Federal University of Bahia, Salvador, Bahia, Brazil
[c] Centro Universitário SENAI CIMATEC, Av. Orlando Gomes, 1845—Piatã, Salvador 41650-010, Brazil
[d] Department of Exact and Earth Sciences, University of the State of Bahia, R. Silveira Martins, 2555—Cabula, Salvador 41180-045, Brazil
[e] Collective Health Institute, Federal University of Bahia, Salvador, Bahia, Brazil
[f] Santa Cruz State University, Ilhéus, Bahia, Brazil
[g] Instituto Federal de Ciência e Tecnologia da Bahia (IFBA), R. São Cristóvão, s/n - Novo Horizonte, Lauro de Freitas, 42700-000, Brazil
[h] The Babraham Institute, Laboratory of Lymphocyte Signalling and Development, Cambridge, United Kingdom
[i] London School of Hygiene and Tropical Medicine, London, United Kingdom

ARTICLE INFO

ABSTRACT

Arbovirus can cause diseases with a broad spectrum from mild to severe and long-lasting symptoms, affecting humans worldwide and therefore considered a public health problem with global and diverse socio-economic impacts. Understanding how they spread within and across different regions is necessary to devise strategies to control and prevent new outbreaks. Complex network approaches have widespread use to get important insights on several phenomena, as the spread of these viruses within a given region. This work uses the motif-synchronization methodology to build time varying complex networks based on data of registered infections caused by Zika, chikungunya, and dengue virus from 2014 to 2020, in 417 cities of the state of Bahia, Brazil. The resulting network sets capture new information on the spread of the diseases that are related to the time delay in the synchronization of the time series among different municipalities. Thus the work adds new and important network-based insights to previous results based on dengue dataset in the period 2001–2016. The most frequent synchronization delay time between time series in different cities, which control the insertion of edges in the networks, ranges 7 to 14 days, a period that is compatible with the time of the individual-mosquito-individual transmission cycle of these diseases. As the used data covers the initial periods of the first Zika and chikungunya outbreaks, our analyses reveal an increasing monotonic dependence between distance among cities and the time delay for synchronization between the corresponding time series. The same behavior was not observed for dengue, first reported in the region back in 1986, either in the previously 2001–2016 based results or in the current work. These results show that, as the number of outbreaks accumulates, different strategies must be adopted to combat the dissemination of arbovirus infections.

1. Introduction

Dengue epidemics have been affecting different regions of Brazil since 1986. More recently, in 2014 and 2015, two new diseases caused by the viruses chikungunya and Zika, respectively, and transmitted by the same vector *Aedes* genus mosquitos have emerged in the country [1,2]. Zika infections have been associated with an increased risk of Guillain-Barré Syndrome and congenital malformations in newborns [1,3–5], while chikungunya infections lead to intense arthralgia and consequent reduction in life quality of those affected by persistent pain after the acute period of the disease [1,6,7].

A complex public health problem arises from the co-circulation of

---

* Corresponding author.
  E-mail address: vivas@ufba.br (J.G.V. Miranda).
  [1] These authors contributed equally to this article.

three different viruses, as they cause specific but also similar symptoms, increasing the difficulty of diagnosing on acute phase and controlling the spread of the diseases between and across different regions. Thus, understanding the dynamics of dissemination of these viruses is of utmost importance.

Various approaches based on the general formalism of complex networks have been proposed and successfully used when studying complex systems such as epidemics, as they reveal aspects of the propagation dynamics not clearly perceived from the series of case records [8–13]. Networks are graphs represented by vertices (or nodes) and pairwise edges connecting them [11], which represent the individual agents and their interaction associated with the phenomenon being studied. In the current case, network nodes represent cities and edges are included according to a relation between the temporal emergence of the diseases (dengue, Zika and chikungunya) observed in the time series. This allows understanding how the cases of each arbovirus in different municipalities are temporally and spatially related. The study of epidemics through networks allows for a better understanding of how they spread and thus help in the possible control of the disease.

Some previous works have already shown the importance of using networks to study dengue spread, which contributed to uncovering the mechanism of dissemination of the dengue virus. Malik et al. [14] studied dengue transmission networks and found that they were characterized by a scale-free type topology. The authors associated this finding to the presence of spreading nodes, on which control policies could be focused at the same time. Simulations on network models were carried out, as in [15]), who made a network model with the purpose of investigating the possible influence of vaccination and vector control on the virus transmission network. Malik et al. [16] developed a network model that simulates possible internal and external factors that can cause or contribute to dengue virus transmission.

Regarding the virus spread on a geographic region, Saba et al. [17] used reported cases from years 2000 to 2009 in the state of Bahia, Brazil, to show how the occurrence of dengue in different municipalities were correlated. Next, by obtaining dynamic networks generated based on this dataset Saba et al. [18] showed how mobility influences the disease dissemination.

Our literature survey detected only two studies about Zika using network models [19,20], but none using chikungunya data. Thus, the main objective of this work is to present a comprehensive study of the spread of the three arboviruses (dengue, Zika and chikungunya) using a time-dependent complex network approach.

In order to study the time dependence of the spreading process within the municipalities' network, we used the concept of Time Varying Graphs (TVG). As a criterion to insert network edges for each time interval we used the Motif-Synchronization (MS) method [21]. In addition, to account for the delay required for the virus to reach other locations, we evaluate the delay time in synchronization between municipalities. This way it is possible not only to insert an edge in the network but also to measure the delay time for which the largest synchronization degree between two series is observed.

Important issues will be addressed in this work, e.g.: i) ability of adopted approach to characterize, quantify, and possibly distinguish differences among the spread dynamics of three arboviruses; ii) the characteristic lag time associated with each of them; iii) existence of relation between intercity distance and the delay time; iv) existence of a set predecessor municipalities acting as hubs for disease dissemination.

Based on dengue incidence data from 2001 to 2016 for the state of Bahia and on the approach described above, Araújo et al. [22] addressed some of these questions, analyzing the delay time in order to set up a model characterizing the spreading behavior. They concluded that the dengue spreading is not directly related to the distance between municipalities, but rather to a temporal relationship with the life cycle of the mosquito and its ability to transmit the disease.

Now we use a unified data set covering reported cases of the three quoted arbovirus from 2014 to 2020, whereby Zika cases started being registered as such only from 2015 on. As before, the networks obtained within this framework characterize and quantify the spread of three different diseases, allowing for uncovering differences and similarities among them. All four issues listed previously will be fully addressed.

In the period 2014–2020, Bahia registered of two major dengue outbreaks, concomitantly with Zika and chikungunya outbreaks between 2015 and 2016 [23–25]. Because of that, in this specific period we conducted a more detailed analysis of the spread dynamics.

The rest of this work is organized as follows: in Section 2 we introduce the basic concepts of the framework used to convert time series into network, namely: TVG, motifs, and MS. As the whole framework has been already used and presented else, we refrain to repeat her all details of the procedure, which can be found in the suggested literature. Section 3 discusses the main features of the data used in our analysis, Results obtained in our work are discussed in Section 4, which is assembled by 4 subsections. Finally, Section 5 closes the work with our conclusions and perspectives.

2. Methods

2.1. Time-varying graphs (TVG)

The TVG approach was used in this work with the purpose of studying the dynamics of arboviruses dissemination, as it allows obtaining a sequence of networks for different instants of time. In this work, the networks depend on the number of reported cases for each municipality as a function of time.

Several authors, such as Flocchini, Mans and Santoro [26], Casteigts et al. [27] and Nicosia et al. [28], contributed to the formalization of this method. A TVG is defined as a set of graphs with a fixed number of vertices, in which edges appear and disappear along the time (see Tang et al. [29], Nicosia et al. [28]) As such, it corresponds to a set of M graphs $\{G_1, G_2, ..., G_M\}$ (Fig. S1), all of which with a fixed number N of vertices, and each G_m in this sequence represents the state of the network at the time tm, with $m = 1,...,M$. Note that the number of edges at each graph G_m depends on the way the TVG is defined. Therefore, it is well possible that, for some G_m, some nodes may not be connected to any other node, i.e., not all G_m correspond to a connected graph. Besides that, each G_m can be analyzed individually with the usual metrics of graph theory, or they can be analyzed jointly, providing an integrated view of the phenomenon that is represented by the TVG.

2.2. Motif-synchronization (motifs and MS)

The MS framework [21] generates a synchronization measure between two time series through a fast evaluation of correlations. To this purpose, it first maps the original series into a series of a small set of different patterns called motifs which, in a second step, allows to searching the time lag between the two series that maximize the synchronization score. It has been recently used to build networks using electroencephalography (EEG) time series [21,30] as well as weekly records of dengue cases [22,31] and COVID [32].

Motifs are different patterns formed by a set of consecutive points extracted from the time series according to a suitably chosen period. They are characterized by the relative point positions and resulting slopes of straight lines between them. The order of a motif is defined by the number of points is made of. For each order, there is a finite set of all relative point positions. Here we consider a sub-set of 6 different motifs of order 3, labeled as M_z, $z = 1, ..., 6$, as illustrated in Fig. 1. The reason for this choice is that it provides a best trade-off between simplicity and ability to identify basic trend changes in a time series.

The number of points generating the motif (motif degree) and the gap between the points (lag), shapes each motif. For motif degree $n = 3$, there are $n! = 6$ possible motifs. The motif time series X_{Mi} may be defined according to the relationship between successive data elements X_i, $X_{i+\lambda}$ and $X_{i+2\lambda}$ as
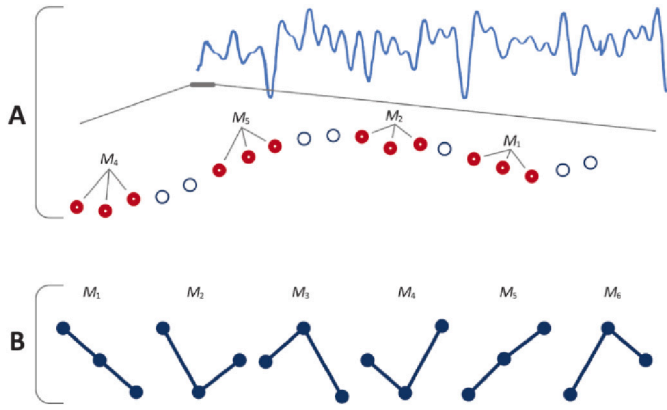
Fig. 1. Illustration of the conversion of time series into a motif series. Panel A shows a time series, a small part of which is enlarged to display the individual points it is made of. It consists of 19 points, which define 17 motifs. Panel B shows some order 3 motifs, defined by a sequence of three successive points. The identification of a motif depends on the relative position of the points it contains. The panel shows only the 6 different order-3 motifs used in this work. Panel A also highlights the process of identifying 4 motifs (from some arbitrary sets of 3 red points), as well as the first 10 motifs in the motif series. (For interpretation of the references to colour in this figure legend, the reader is referred to the web version of this article.) (Figure adapted from Li and Ouyang [49])

$$
X_{M_i} = \begin{cases} 1, if\, X_i > X_{i+}, X_{i+} > X_{i+2}, X_i > X_{i+2} \\ 2, if\, X_i > X_{i+}, X_{i+} < X_{i+2}, X_i > X_{i+2} \\ 3, if\, X_i < X_{i+}, X_{i+} > X_{i+2}, X_i > X_{i+2} \\ 4, if\, X_i > X_{i+}, X_{i+} < X_{i+2}, X_i < X_{i+2} \\ 5, if\, X_i < X_{i+}, X_{i+} < X_{i+2}, X_i < X_{i+2} \\ 6, if\, X_i < X_{i+}, X_{i+} > X_{i+2}, X_i < X_{i+2} \end{cases} \quad (1)
$$

where X_{Mi} is the element of the motif series and λ is the motif lag.

After converting all data series into a motif series, the correlation degree between two series X and Y at time t is defined by

$$
Q_{XY_t} = \frac{max\{c_{XY_t}, c_{YX_t}\}}{L_M} \quad (2)
$$

where L_M is the length of the sliding synchronization window, and c_{XYt} and c_{YXt} are defined by.

$$
c(X_M, Y_M)_t = c_{XY_t} = max\left\{ \sum_{i=1}^{L_M} J_{t+i}^{\tau_0}, \sum_{i=1}^{L_M} J_{t+i}^{\tau_1}, ..., \sum_{i=1}^{L_M} J_{t+i}^{\tau_{máx}} \right\}, \quad (3)
$$

where

$$
J_i^{\tau} = \begin{cases} 1, if\, X_{M_i} = Y_{M_{i+\tau}} \\ 0, otherwise \end{cases} \quad (4)
$$

We see that $J_i^{\tau} = 1$ or 0 identifies whether the motifs M_{X_i} and $M_{Y_{i+\tau}}$ in the series X_M and Y_M are coincident or not. Thus, c_{XY_t} corresponds to the largest number of times in which a motif Mz appears in the Y series after appearing at time t in the X series within a window of width L_M, for a fixed value of τ_i. The sums in the argument of the max operator in eq. 3 are bounded between 0 (when all J's are 0) or L_M (when all J's are 1). Therefore, $c_{XYt} \in [0, L_M]$ and $Q_{XYt} \in [0, 1]$. The sums in Eq. (3) cover an interval of time lags τ_i running from no delay time $\tau_0 = 0$ up to a suitably chosen maximum delay $\tau_{max} = \tau_n$ (Fig. 2), which represents a n-point shift ahead of the moment where the motive Mz occurred in X. In brief, c_{XY} will be the largest value of the number of identical motifs in a window of length L_M, for values of τ in the interval $[0, \tau_{max}]$.

On the other hand, a synchronization direction q_{XY_t} can be defined after evaluating c_{XY_t} and c_{YX_t} using

$$
q_{XY_t} = \begin{cases} 0, if\, c_{XY_t} = c_{YX_t} \\ sign\,(c_{XY_t} - c_{YX_t}), if\, c_{XY_t} \neq c_{YX_t} \end{cases} \quad (5)
$$

It is possible to see that the value $q_{XY_t} = 0$ indicates no preferred direction; while 1 and -1 indicate that motifs in X are more likely to precede those in Y or vice versa. Here we anticipate that $q_{XY_t} \neq 0$ for the large majority of X, Y and t, indicating the directed character of our TVG networks. This feature makes it possible to identify those cities that most constantly act as spreaders, being responsible for infecting other municipalities.

2.3. Network construction

The networks that form each arbovirus infection TVG are formed by nodes representing municipalities while, for each instant of time t, the
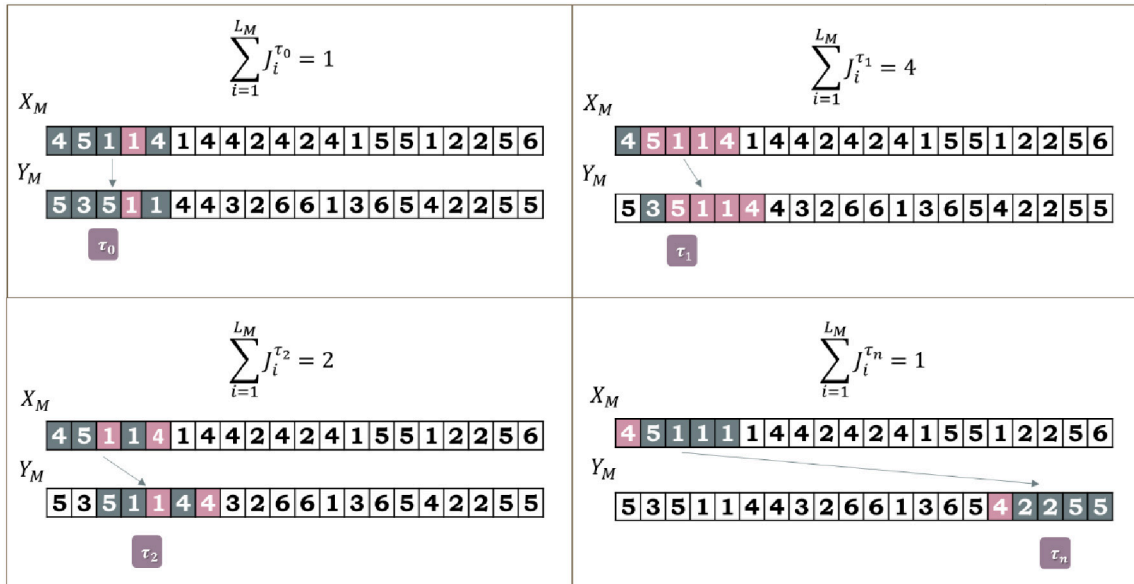

Fig. 2. Sum of simultaneous appearances of motifs for different delay times. Each number in this series refers to one of the motif patterns shown in the Fig. 1.

edges are inserted according to the synchronization index Q_{XY} defined in Subsection 2.2. A synchronization length $L_M = 5$, corresponding to 5 week intervals, was selected for all networks. A 5 weeks interval was the smallest window that still kept a functional meaning, given the typical time scale of the disease spreading. The step-by-step TVG construction [21] proceeds as follows: (i) transform the time series of reported cases (Fig. 3A) into motif time series (Fig. 3B). Then, at each time step t, (ii) evaluate the synchronization degree by counting how many times a motif Mz in series X at time t appears in the time series Y in a L_M sliding window for different delay times τ_i. The degree of synchronization and the delay time $\bar{\tau}$, at which the maximum synchronization between the series of motifs was observed, are recorded. (iii) build the association matrix S_t with elements s_{ij} representing the degree of synchronization between vertices i and j (Fig. 3C); (iv) transform the matrix S_t into the network adjacency matrix A_t (Fig. 3D) by a filtering procedure defined by a suitably chosen threshold σ_{th}, according to

$$a_{ij} = \begin{cases} 1, if\ s_{ij} \geq \sigma_{th} \\ 0, otherwise \end{cases} \tag{6}$$

The threshold σ_{th} is obtained in a procedure where the data from the time series shuffled and subsequently used to construct new networks. Then, σ_{th} corresponds to a 1 % chance of the original network being randomly selected. In this study we assumed σ_{th}=0.9 so that edges between nodes will be allowed only when a large enough synchronization of 90 % or more motifs has been reached. The inserted edges will be associated with the delay time value τ corresponding to the largest obtained synchronization.

The synchronization between two case-motif series i and j is evaluated, at each time t, over a time window of length $L_M = 5$ epidemiological weeks, which leads to a maximum of $M = T - 6$ synchronized values, where T indicates the number of points in the time series. This value of M results from the fact that seven consecutive weeks are required to identify the edges that are present in each individual network in the TVG. Within this procedure, the obtained networks for any time $3 < t < T - 3$ depend on data records from seven successive weeks t' with $t - 3 \leq t' \leq t + 3$.

Once the network adjacency matrix A_t is completed, the construction of the TVG proceeds by shifting the sliding window of length L_M one time step forward and repeating the above procedure to evaluate A_{t+1}. The values of the network parameters τ_{max}, σ_{th}, and L_M used in Araújo et al. [22] for the construction of dengue networks were taken as guidelines to specific choices made in this work.

For the purpose of focusing the analysis to some specific periods, we used different values of τ_{max} but, in most cases, the value $\tau_{max} = 10$, which implies in looking for maximum synchronization up to 10 steps ahead of the first window. As one time step corresponds to one week, such a maximum delay is sufficient to detect correlated events well displace in time but not exceeding the characteristic time interval of the outbreaks. This choice is further empirically corroborated by analyzes based on the number of maximal synchronizations in the networks that are observed at the delay time $\bar{\tau}$ value for values of τ_{max} in the range 40–50.

The time dependent networks in the TVG approach (Fig. 3E) can be aggregated to provide a global picture of the underlying process it describes. To this purpose we consider the aggregated static network (ASN) (Fig. 3F), which is a weighted network with the same nodes as those in the TVG, where the weight of each edge b_{ij} is given by the number of times that a directed edge from node i to node j appears in the TVG networks.

To estimate the distances between the municipalities, necessary for identifying the spatial dependence of the delay time, we considered the latitude and longitude data provided by the Brazilian Institute of Geography and Statistics [50]. These coordinates were then converted into the Mercator's Universal Transverse two-dimensional Cartesian coordinate system (UTM). It was designed to project a three-dimensional

sphere onto a two-dimensional map, while the geodesic coordinate system – latitude and longitude – are used to locate places on the Earth's three-dimensional surface [33–35]. The unit of measurement of the UTM is the meter and this was the reason for choosing this coordinate system to calculate the distance between the municipalities.

3. Data

The networks were built based on public and non-identified data obtained from the Notifiable Diseases Information System of Brazilian Ministry of Health (Sistema de Informação de Agravos de Notificação – SINAN, in Portuguese) [36]. The used dataset contains the daily reports of notified dengue and chikungunya cases for all municipalities in the state of Bahia from 2014 to 2020, as well as those of Zika from 2015 to 2020. Based on original information on date of onset of symptoms and residence places, time series of reported cases for the three types of arbovirus infections were obtained for each municipality. Finally, daily counts were aggregated on a week basis, giving rise to the number of weekly reported cases, which were the input data for this work, and the time step t corresponds to the epidemiological weeks.

The state of Bahia, Brazil, has an area of 567,295 km^2 and is divided into 417 municipalities, mainly connected by a land transportation network [37]. Bahia's territorial area is larger than the areas of countries such France (543,965 km^2). Besides, Bahia has specific climatic conditions such as varied precipitation, which may justify the non-homogeneous number of cases of arboviruses infections as climate is usually associated with disease propagation [38].

4. Results and discussions

We start by considering the histograms in Fig. 4 where, for each of the three TVGs, each point represents the total number of edges that were inserted in any of the corresponding time-varying networks at a certain delay time. All of them are characterized by large peaks at low values of delay time, which are markedly reduced around $\bar{\tau} = 10$. A further important feature of these histograms is the presence of a second broad and much less intense peak at later times, i.e., ~ 34 weeks for Zika and chikungunya and 48 weeks for dengue. The found value $\bar{\tau} = 10$ justifies selecting also $\tau_{max} = 10$ in most of our analyzes, albeit it was necessary to use other values of τ_{max} when investigating the relation between the characteristic delay time for disease spreading and inter node distance using network indices. In such cases, the investigation should cover small to large delay times. The histogram in Fig. 4 runs up to $\bar{\tau} = 50$, so as not to exceed the period of 1 year.

The main results are addressed in the next four different subsections. In the first one, the main network features obtained within the MS frameworks are discussed and, in the sequence, the characteristic delay time $\bar{\tau}$ for maximal synchronizations. The third subsection brings a detailed analysis of the spatial dependence of the delay time with maximal synchronization. Finally, subsection four is presents the ranking of spreader cities, i.e., those that mostly play the role of transmitting the infection to other network nodes.

4.1. Main features of the motif-synchronization networks

In accordance with the methodology discussed in the previous section, here we present some important features of the networks obtained within the TVG framework that reveal relationships among the number of arbovirus cases in the municipalities. The results, which can be associated with the phenomenon of disease spreading, turn it possible to explicit such relationships based on the obtained values of time delays for synchronization. Within this subsection, all networks were generated using $\tau_{máx} = 10$.

The main outputs of our analyses are: (i) the correlation between the number of cases and the total number of edges of the networks in the TVGs; (ii) a comparison between the evolution curves of the averages of
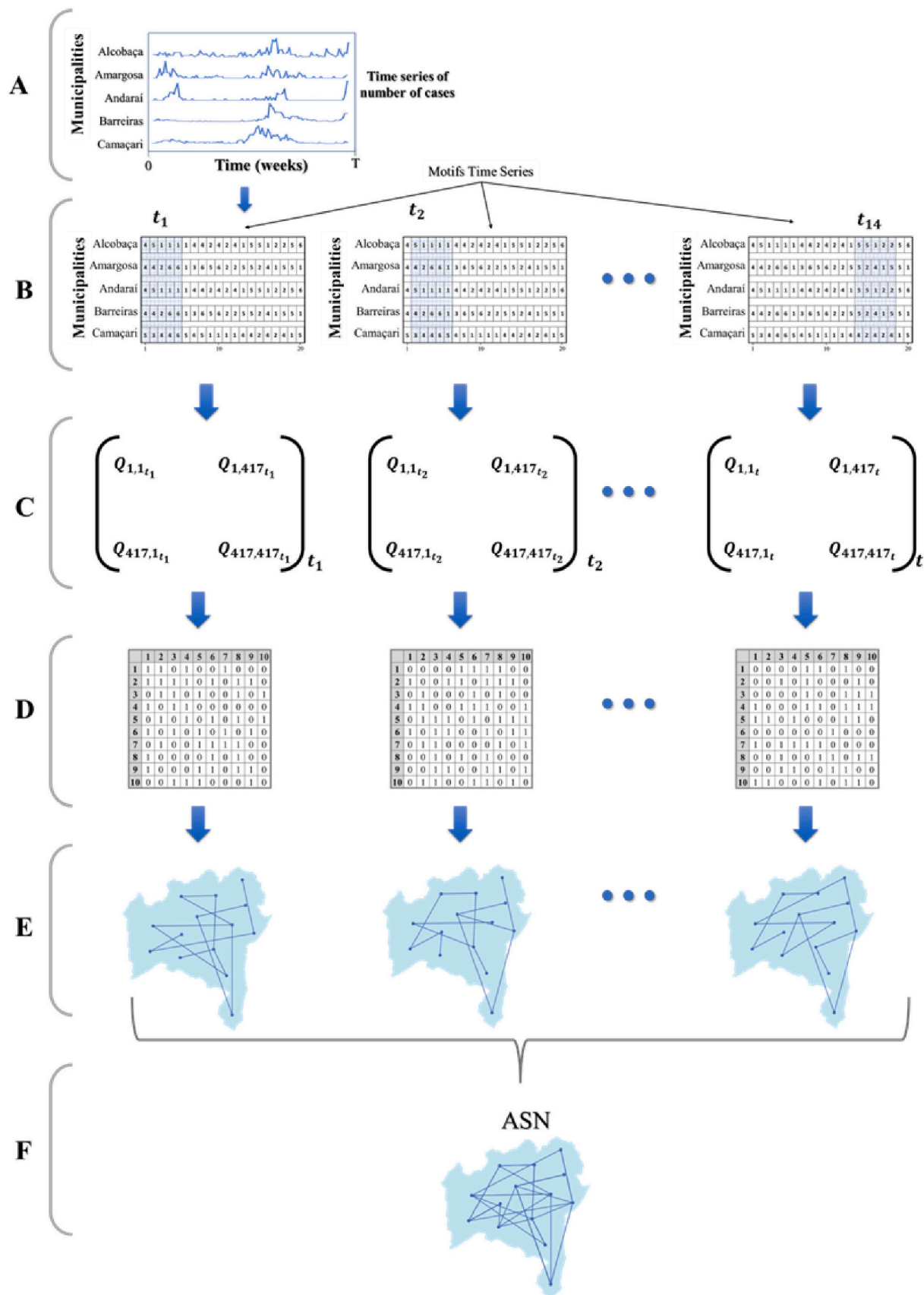
Fig. 3. Scheme of the construction of networks. A) Time series of weekly cases. It will be converted into Motifs time series. B) Time series of motifs and the size sliding windows in which the synchronizations of each vertex pair will be calculated. C) Synchronization matrix, in which each element represents the degree of synchronization of each vertex pair. D)Matrices of correlation with the representation of network connections L_M. E) Representation of the networks created for each moment of time (TVG). E) Aggregate Static Network, in which it has the information of the connections of all TVG networks.
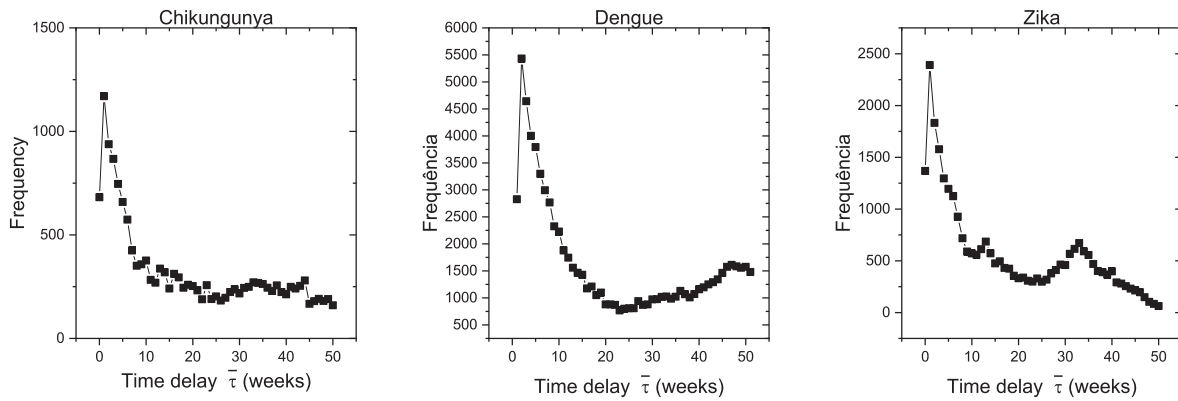
Fig. 4. Delay time histograms for the three TVGs. The horizontal axis range from $\bar{\tau}=0$ (when there is no delay between the time series) up to $\bar{\tau}=50$, which represents a delay equivalent to 50 weeks in the synchronization of the case series.

cases with the weighted degree of these networks.

The correlation between the number of cases and number of edges can be appreciated in Fig. S2, where each point condenses the information for a single week. The number of cases is performed over the weekly registered cases of all municipalities, while the number of edges counts how many edges appear in the corresponding TVG network for the same week. The corresponding Pearson correlation values for each arbovirus are presented in Table S1.

The obtained values are high (> 0.89) for the three arboviruses, indicating that an overall increase in the number of cases of the diseases in the different municipalities is associated to an increase in the number of networks edges. In the work by Araújo et al. [22], such an analysis was carried out to test the hypothesis that the TVG networks within the motif synchronization method could characterize the spread of dengue in the municipalities. The obtained large correlation between the variables leads the authors to conclude that the enounced hypothesis was valid. Thus, the results in Table S1 for dengue, Zika, and chikungunya provide support to the hypothesis that evaluating the properties of TVG networks is a good way to characterize the spread of these arboviruses.

A comparison between the time series for the average degree of the network and the average of cases is presented in Fig. 5. The average of cases was obtained from the average number of cases in all municipalities in the period of 7 weeks.

The first observation is that the time series of the average degree and the average of cases show very similar patterns. This result is closely related to those in Fig. S2, once the previously discussed increase in the number of networks associated with the increase of the number of cases will naturally increase the average node degree of the network. As expected, the high values of the R-Pearson coefficient in the fourth columns of Table S1 attest the presence of strong correlation (> 0.92). The

increase in the average degree of the network when there is an increase in the average of cases, suggests that the outbreaks detected in most municipalities are connected with each other.

In Table 1 we indicate the months in which the largest numbers of arbovirus cases occurred, and highlight in orange those peaks with the corresponding largest values of the network average degree in the graphs in Fig. 5.

The peak positions shown in Table 1 indicate a fairly periodic seasonal pattern for the dengue occurrences during the whole investigation period, with largest intensities in 2015 and 2016. Similarly, the network approach also assigns largest value of average node degree. However, the major outbreaks of the other two arboviruses, concentrated in 2015 and 2016, were far less likely to exhibit the same seasonal dependence in the corresponding curves of Fig. 5.

Table 1

Months and years with largest numbers of the average degree graph in Fig. 5. The months where outbreaks attained highest values (peak tips) are highlighted in orange.

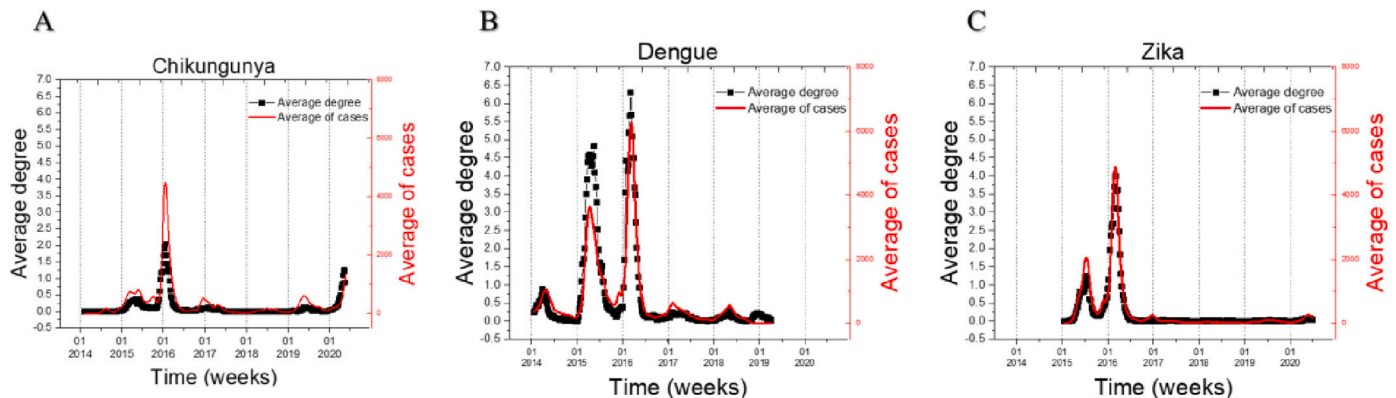|	Peak positions				
Chikungunya	May/2015	Jan/2016	Dec/2016	May/2019	May/2020
Dengue	Mar/2014	Apr/2015	Mar/2016	Feb/2017	May/2018
Zika	Jul/2015	Mar/2016	Dec/2016	May/2020	

Fig. 5. Time series of average of cases and mean degree of networks.

We further observe that the time interval between the largest outbreaks of chikungunya and Zika was 34 weeks, which coincides with the second peak observed in the time delay histogram in Fig. 4. What concerns dengue, a second peak in the delay time histogram was observed at ~48 weeks, which is much closer to the seasonal periodicity commented before. The presence of such shallow peaks at in Fig. 4 should not be interpreted as resulting of the transmission from one specific city to the other one over such a large period, but as an evidence that the spreading process follows similar patterns at each new outbreak.

Table S2 details the initial and final months of the two main 2015 and 2016 outbreaks for the three arboviruses, which cover approximately 80 weeks. In Sub-section 4.3 we will analyze some special features presented by each of them, by considering the dependence between the obtained time delay for the synchronization and the intercity distance.

4.2. Characteristic delay time

In this sub-section we discuss specific features of the delay time in the synchronization of arbovirus networks, as an alternative way to characterize the time dependence of the disease spread over the considered region. In such way it is possible to test the hypothesis that the synchronization delay time is somehow related to the time that the viruses take to be transported between cities.

Thus let us consider again the delay time histograms in Fig. 4 which, in order to investigate the longest possible delay of synchronizations, were obtained for TVG networks built with $\tau_{max} = 50$ weeks, in such way that $\bar{\tau} \in [0,50]$ weeks. There we see that most edges have a delay time of 1 week. Araújo et al. [22] estimated that the most likely delay time for dengue networks was around 2 weeks, which is consistent with our results indicating that the most frequent delay times were observed for $\bar{\tau} = 1, 2,$ and 3.

These authors also emphasize that the obtained value $\bar{\tau} = 2$ may be related to the dengue transmission cycle between individuals, as supported by the current literature indicating that the extrinsic incubation period, which is the period when the mosquito bites an infected person and begins to become infectious, varies between 8 and 12 days [39,40]. The intrinsic incubation phase, which represents the period between the individual being bitten and the onset of symptoms [39], ranges from 4 to 10 days for dengue [40], 3 to 14 days for Zika [41] and 1 to 12 days for chikungunya [6]. Although the extrinsic and intrinsic incubation periods vary for each arbovirus, we can consider all arboviruses together and consider that this period can vary between 9 and 24 days, which encompasses the 2 to 3 weeks period mentioned by Araújo et al. [22]. Due to the resolution of the time series, the delay time of 1 week within the TVG approach actually ranges from a delay of 7 to 13 days, so that $\bar{\tau} = 1$ in network synchronization is in accordance with the intrinsic and extrinsic incubation periods.

To uncover the origin of other smaller peaks observed around 34

weeks for Zika and chikungunya, and 48 weeks for dengue, we built similar histograms as those in Fig. 4 whereby only the delay times corresponding to the period comprising the two main detected outbreaks were taken into account. This corresponds to an 80 week interval between the last months of 2014 and June of 2016, as indicated in Table S2. The results in Fig. 6, indicating that the secondary peaks have been comparatively highly magnified, indeed suggest they were associated with the time interval covered by the two largest peaks in Fig. 5. Therefore, taking into account the characteristic times for intrinsic and extrinsic incubation periods quoted above, we conclude that the synchronizations among the motifs with such large values of $\bar{\tau}$ result from the superposition of two outbreaks and, as such, should not have significance for the disease spread in a single outbreak.

4.3. Spatial dependence of delay times

Here we investigate the relationship between the geographical distance between the cities represented by nodes and the synchronization delay time used as a condition for including a network edge between them. The results aim confirming or denying the existence of a growing monotonic relationship between these two measures associated with the TVG networks. The delay time in synchronizations would then be greater as the distance between the municipalities increases, due to the larger time required for the virus to spread from one city to the other. The results were obtained for $\tau_{max} = 40$ weeks.

The graphs in Fig. S3 show the average delay time as a function of the intercity distance, whereby each point congregates the contributions of intercity distances within a bin of width 10 km. The results, which cover the entire available periods in the data set, namely, from 2014 to 2020 for dengue and chikungunya and from 2015 to 2020 for Zika, fail to indicate a clear monotonous relationship between the variables.

However, one must consider that these results are actually average values, as they account for delay times stemming from a large time interval, and that relevant details of individual outbreaks may have been severely blurred. To clear out this issue, we obtained similar results based on the data covering smaller time intervals, as those including the two large outbreaks characterized in Table 1 and Fig. S4, in which they are identified as Outbreak 1 and Outbreak 2, respectively. Table 1 shows the periods of these two outbreaks for each of the arboviruses. The analysis of these two periods was done by selecting the networks of the first outbreak and the networks of the second outbreak separately.

For each event characterized as Outbreak 1 and 2, we show in Figs. 7, S5, S6 and S7 the corresponding graphs of delay time vs. intercity distance for the three TVG networks, whereby in Fig. 7 we considered $\tau_{max} = 40$ only, while in Fig. S5, S6 and S7 we let τ_{max} assume different values in order to illustrate the role played by this parameter in establishing a dependence between delay time and intercity distance. Note that, when $\tau_{max} = 40$–9 months, the networks in the first outbreak admit synchronizations between weeks which belong already to the period of
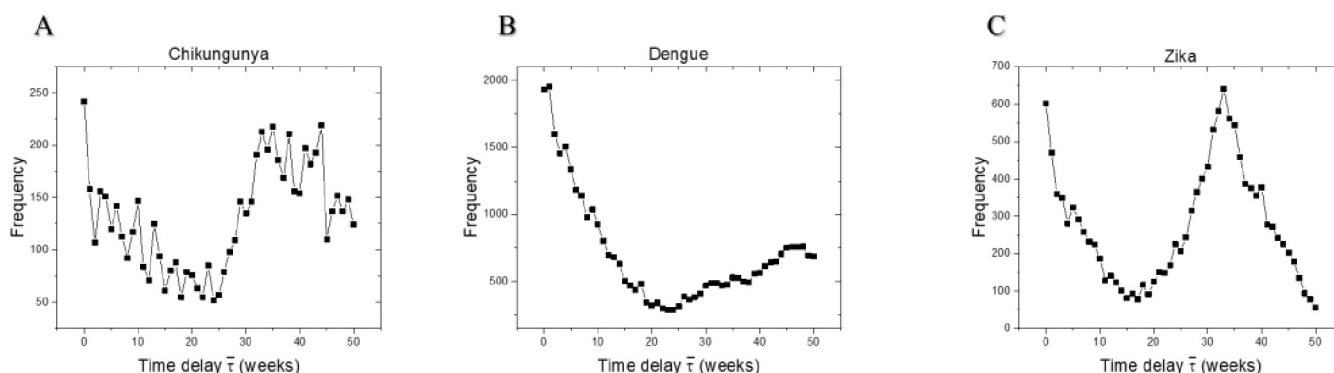

Fig. 6. Histogram of delay times for the period comprising the largest outbreaks in Fig. 5. A) Chikungunya. B) Dengue. C) Zika.
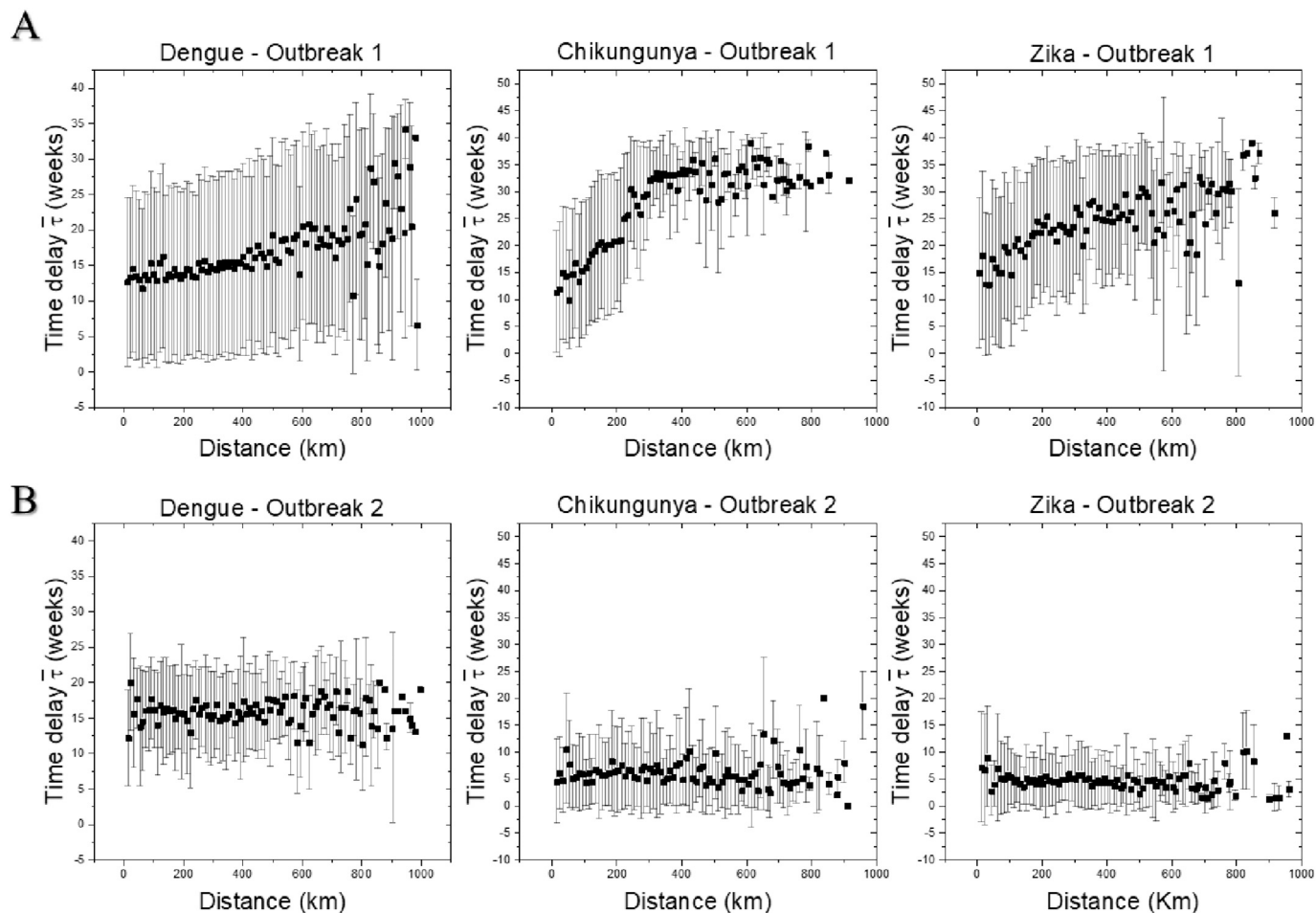
Fig. 7. Delay time vs. time graphs. Distance to dengue, Zika and chikungunya networks. A) Outbreak 1 period networks. B) Outbreak 2 period networks.

the second outbreak (Table 1). Similarly, networks in the second outbreak may include synchronization with data 40 weeks ahead which, as indicated in Table 1, do not reach the next peak. When using smaller values as $\tau_{max} = 10$, the networks from the first outbreak may include only small amount of data in the beginning of the second outbreak, so that it is more likely to progressively obtain information from single isolated outbreaks. In summary, in the following analyses, we consider $\tau_{max} = 40$ in order to study the spatial dependence of delay time, whereas $\tau_{max} = 10$ was used when we wanted it to be an isolated analysis of outbreaks.

Fig. 7 shows the results for each arbovirus and outbreaks with $\tau_{max} = 40$ weeks. During the period comprising the first outbreak, identified as Outbreak 1 in Fig. 7A, it is possible to identify a monotonous increase of the delay time with the intercity distance for the three arboviruses. For dengue, with the smallest increase tendency, we further observe that the error bars are too large, so that the inference of a spatial dependence of the delay time may be questionable. However, in the case of Zika and chikungunya, the spatial dependence of the delay time is more strongly evidenced. On the other hand, results for the networks in second outbreak period in Fig. 9B do not show identifiable spatial dependence of the delay time.

To clear out further aspects of the relationships between time delay and intercity distance (Fig. 7), we developed three different strategies and used them to analyze the data for the period of the two largest outbreaks. In first place we generated TVG networks for delay times $\tau_{max} = 5, 10, 20, 30$ and 40 (Fig. S5, Fig. S6 and Fig. S7), making it is possible to see whether more distant municipalities would be connected in networks with smaller delay times. Next, we identified the municipalities that appeared in the TVG networks of each outbreak, with special attention to those that were present in second one but not in the first. This way it was possible to identify virus spread to municipalities that occurred only during outbreak 2. Finally, we used the framework of aggregate static networks ASN to analyze the entire period comprising the two main outbreaks.

The results for different values of τ_{max} are shown in Figs. S5, S6 and S7. In the chikungunya networks (Fig. S5) connections appear only between the closest municipalities when $\tau_{max}=5$. As its value progressively increases, new edges connecting more distant municipalities appear. This picture is consistent with the facts that the chikungunya virus has arrived in Bahia in 2013–2014 and that the analyzed outbreaks were the first large observed occurrences, when the virus reach municipalities far apart the first infected ones, gradually spreading throughout the state.

The dengue networks (Fig. S6) do not show this pattern, as networks with $\tau_{max} = 5$ includes connections among distant municipalities. The same occurs in the Zika networks (Fig. S7), with connections among distant municipalities connected even for short delay times. However, the resulting patterns for the corresponding networks when $\tau_{max}=30$ and 40 are different from each other: for the Zika networks the points are aligned along an increasing line with large slope, whereas such a tendency can hardly be detected for dengue.

The chikungunya and Zika viruses have been presumably been introduced in Brazil in 2013 and 2014 (a relatively short delay ~1 year), when the country hosted international sport events [5,24,42,43]. As it took a while for each of them to be transported to municipalities far away from the places where they were introduced, the relevant differences between the patterns in Fig. S5 and S7 are quite surprising. A

possible explanation is the fact that clinical symptoms of Zika are very similar to those of dengue. So, it may be that, upon the virus being introduced in Bahia, the first infected individuals were not reported as Zika cases, while the first reported cases – from 2015 onwards [3] – only happened when the virus had already spread into several regions.

The identification of municipalities where chikungunya and Zika had not been reported until the start of Outbreak 2 offers a way to account for the continuity of the spreading process. Table S3 shows the percentage of municipalities at least one case in the corresponding outbreaks, as well as the percentage of municipalities in which cases were reported only in Outbreak 1 or in Outbreak 2.

Table S3 reveals a significant increase in municipalities with cases of chikungunya (from 51 % to 80 %) and Zika (from 58 % to 86 %) from Outbreak 1 to Outbreak 2, as well as a large number of municipalities with cases first reported in Outbreak 2 (42 % for chikungunya and 36 % for Zika). On the other hand, dengue shows similar percentage of municipalities with at least one case in each of the outbreaks (94 % in Outbreak 1 and 95 % in Outbreak 2), and only a small amount (5 %) of municipalities with cases in Outbreak 2 but not in Outbreak 1. These results support that chikungunya and Zika went through a spreading process among the municipalities from the end of 2014 to June of 2016, while dengue virus were already present in the large majority of the municipalities.

Finally, we obtained and analyzed the ASN's corresponding to the periods comprising the two main outbreaks (Fig. S8). In this process we considered $\tau_{max} = 10$ in such a way to avoid synchronization between distinct outbreaks and to restrict the analysis to each indicated period. The chikungunya networks show that, during the first outbreak (Fig. S8A), only the closest municipalities are connected to each other. This connection pattern expands to the other municipalities after the second outbreak (Fig. S8B), supporting again the scenario that the virus was found initially in a relatively small region and spread later to more distant places. Similar features are also displayed by the Zika networks (Fig. S8C and S8D), i.e., the edges connecting mainly municipalities in the northeast part of the state during the first outbreak and spread over time to the central, west and south regions.

The dengue networks for the first and second outbreaks (Fig. S8E and S8F) include short and long distance connections among municipalities in all state regions, a completely different pattern when compared with the recently introduced arbovirus. Therefore the three aspects revealed by Figs. Fig. 7, S5, S6 and S7 and Table S3 consistently indicate that dengue, which established in the whole state mode than 25 years ago, has lost, the spatial diffusive character still identified in the first Zika and chikungunya outbreaks.

In a previous work using the TVG approach, Araújo et al. [22] identified the absence of any dependence between delay time and intercity distance in dengue networks for the period 2001–2016. They raised the hypotheses of a non-local virus spread caused by the rapid intercity people commuting through modern transport systems, which allows people to move great distances and causing virus transmission to occur almost simultaneously in different regions. Results found by Saba et al. [18] also highlighted the role played by the transport system on the spread of dengue among the municipalities.

However, it is also necessary to consider that dengue, being established in the region for a long period, has become a disease of local dissemination, irrespective of the occurrence of further spatial dissemination by the transport system. This would require the presence of a small number of individuals carrying the dengue virus in a large number of cities in such a way that, when there is an uncontrolled increase in the number of mosquitoes cause the local number of dengue cases increases in each region. It is known that seasonal climatic conditions [40], e.g., periods of great heat and humidity, highly favor the appearance of virus transmitting mosquitoes.

To have additional indications on the origin of the different dependence patterns, we analyzed the chikungunya and Zika outbreaks occurred in 2020 (see Fig. S3), respectively 7 and 6 years after they were

introduced in Brazil. Fig. S9A and Fig.S9 show the corresponding chikungunya and Zika ASNs. In order to follow the pace at which new connections are introduced into the networks, we repeated the analysis for different values of $\tau_{max} \in [0,10]$.

The main features in the chikungunya networks (Fig. S9A) is the presence of short and long distance connections for all τ_{max} values, even for $\tau_{max} = 0$ and 2. Differences observed when its value increases refer mostly to an increase in the number of edges, irrespective of their short or long distance character. In this sense, it differs from the evolving patterns in Fig. S8A and B corresponding to the years 2014/2015 and 2016. The same scenario is valid for the Zika networks shown in Fig. S9B. These analyses support hypothesis that, once the arboviruses establish themselves in a given region, the emergence of new outbreaks does not follow those features associated with a spatial spreading of a causing agent.

4.4. Identification of spreading out-hubs

Following a remark on the directed character of the TVG networks in Subsection 2.2, here we analyze the role played by out-hub municipalities, i.e., those with largest number of outgoing edges in the TVG networks. Once infections in such cities usually precede those that receive their out-edges, they play key role in the disease spreading. Paying greater attention to their outbreaks might help reducing the arboviruses cases in the state.

In the TVG networks using motif-synchronization network construction, whenever a vertex is connected with another one with a delay time $\overline{\tau} > 0$, there is a directed edge from the predecessor vertex to the successor vertex. Thus we proceed by identifying the vertices that acted as predecessors for largest number of TVG networks.

We start with the ASN and filter out the undirected edges, i.e., edges with zero delay time are not included for the purpose of investigating predecessor municipalities. The so obtained directed ASN undergoes a new filtering process to select the edges with the largest weights. The used criterion is that they must be larger than a threshold value, corresponding to the weight average plus two standard deviations:

$$b_{th} = \langle b_{ij} \rangle + 2\zeta$$

where ζ indicates the standard deviation of the ASN weight.

The set of edges with $b_{ij} \geq b_{th}$ define a subnetwork called HUBASN, a ASN subnetwork formed by its out-hubs only. For each municipality i we define the total weight $W_i = \sum_j b_{ij}$ and the source frequency θ_i which counts the number of values of j for which $b_{ij} > 0$.

Table S4a lists, in descending order, the municipalities with highest source frequency θ_i, i.e., those that are predecessors of a very large number of municipalities. Table S4b shows, also in descending order, the municipalities with largest total weights W_i.

Looking the other way around, in Table 2 we list those municipalities that simultaneously act as predecessor for the three arboviruses for the entire period networks.

Looking the other way around, in Table 2 we list those municipalities

Table 2
List of municipalities present simultaneously in the three arboviruses rankings in Table S4.

Municipalities present simultaneously in the three arboviruses – Source frequencies θ_i	Municipalities present simultaneously in the three arboviruses – Total weights W_i
Camaçari	Camaçari
Feira De Santana	Feira de Santana
Ilhéus	Ilhéus
Itabuna	Itabuna
Salvador	Salvador
Serrinha	Serrinha
Simões Filho	Simões Filho

Table 3

Lists of the municipalities with the largest values of W_i as function of θ_i for each of the arboviruses.

Chikungunya			Dengue			Zika		
Municipalities	θ_i	W_i	Municipalities	θ_i	W_i	Municipalities	θ_i	W_i
Feira de Santana	17	147	Itabuna	27	312	Campo Formoso	25	174
Salvador	17	137	Salvador	27	246	Salvador	22	175
São Francisco do Conde	13	89	Barreiras	27	210	Itabuna	21	176
Santaluz	13	74	Vitória da Conquista	24	189	Simões Filho	20	129

that simultaneously act as predecessor for the three arboviruses for the entire period networks. We conjecture they constantly suffer the presence of a large vector population, a necessary condition to transmit all three arboviruses. Besides being the most populous in Bahia, they are known to be hubs in the state's transport network, with a large commute movement of people from different locations.

A better display of the most significant predecessor municipalities in the networks for each of the arboviruses can be observed in plots of W_i as function of θ_i, as highlighted in Fig. S10.

Table 3 identifies the four highlighted municipalities for each arbovirus in Fig. S10. They had a greater relevance for the spread of different viruses during the period of study, particularly during the 2015 and 2016 outbreaks that concentrated the majority of reported cases. It is interesting to observe the important role played by Santa Luz (chikungunya) and Campo Formoso (Zika) during the corresponding outbreak periods, although they have relatively small population as compared to other cities in the table. Another fact to note is that, with exception of the state capital Salvador and the regional center Itabuna, the other municipalities appear just once in the tables. Although we found seven municipalities appear simultaneously in the top 20 ranking, just one of them remains present in the top 4 ranking. It is to be expected that the same municipalities responsible for the spread of each arbovirus were the same. The hypothesis is that when the virus establishes itself in a certain region, it is predominant, and there cannot be outbreaks of different arboviruses in the same locality. This hypothesis can be tested using a model in future work.

Despite the importance of identifying the predecessor municipalities for the different arboviruses, the municipalities of the Table 3 were the most important ones for the period studied (2014 to 2020), but may not characterize other periods. Therefore, the municipalities contained in Table 3 are places where it is important to maintain surveillance, in terms of vector control and in the event of an increase in cases, as they are municipalities that presented the highest transmissions regardless of arboviruses.

5. Conclusions

In this work we analyzed the transmission of arboviruses – dengue, Zika and chikungunya – across cities in a bounded geographical focusing on the occurrence of cases in different places and the delay time between these occurrences. We use the motif-synchronization method, which allows for the synchronization of time series for different delay times.

This methodology, which was already used to analyze dengue data [22], was applied in this work to study new data for the three arboviruses in the period 2014–2020. Our results estimate the synchronization delay times, their temporal dependence, and identifies the spatial characteristics playing key role in the spreading processes of the different arboviruses.

A characteristic delay time of 1 week in network synchronizations was found to be highly compatible with the individual-mosquito-individual transmission time. Despite the difference to the reported

delay time of 2 weeks observed previously [22], the obtained histogram of time delay occurrence assigns a large peak covering 1–2 weeks range in both works.

The networks showed different spreading processes for arboviruses depending on the period studied. For the period 2015 and 2016, dengue virus was already present in all municipalities, in contrast with the Zika and chikungunya viruses, which resulted in a diffusion-like pattern across the municipalities. The results obtained for Zika and chikungunya in the year 2020 reveal a pattern that is approaching that of dengue, showing that they were already scattered in different regions, even at the beginning of the outbreak of that period. Other studies have used spatial methods to explain the spread of arboviruses within municipalities, thus much smaller spatial areas, also established that the spread of arboviruses occurs to neighboring locations mostly by diffusion [44–48], which corroborates our results.

The results show that the intercity transmission of diseases through the displacement of people and mosquitoes is one of the factors that influence the increase in cases in different regions, especially when it comes to a recent disease. But it was seen through the analysis of the spatial dependence of the time delay that this process takes time, as the greater the distance from the epicenter of the outbreak, the longer the time for these viruses to arrive in each region. However, once it is established, as mentioned above, other factors seem to be more relevant for the outbreak of these arboviruses in each region, such as climatic conditions, ineffective and insufficient vector control measures, population density and bad sanitation. These results suggest that different combat strategies are essential on the stage of dissemination of each disease in different regions. For a recent disease, when population is naïve, controlling the flow of people in different regions can become an effective measure, but when diseases become established in some places, the mobility of people is only one factor on the dynamics of transmission of arboviruses. It is also important to consider that although dengue virus has been circulating in Bahia since the 1980s, there are four serotypes and constant population replacement. For chikungunya and Zika, until 2014 and 2015 the population was completely naïve, offering a large number of susceptible that collaborated in the transmission of the disease.

The methodology used made it possible to identify the municipalities that proved to be the main predecessors in the synchronizations and the identification of these epicenters constitutes important information to surveillance services, to intensify the vector control measures, avoiding new outbreaks and epidemics in neighboring areas. The predecessor municipalities common to the three arboviruses were identified - which are municipalities that must be associated with a high infestation of the vector, naïve population, high population density, absence or insufficient control measures and bad sanitation. We also identified the municipalities that were the most predecessors for each of the arboviruses by periods, but may not characterize that they were the most important for other periods.

Funding

This work is supported by the Center of Data and Knowledge Integration for Health (CIDACS) through the Zika Platform- a long-term surveillance platform for the Zika virus and microcephaly, Unified Health System (SUS) - Brazilian Ministry of Health. ESP is funded by the Wellcome Trust (grant number 213589/Z/18/Z). The work was partially supported by the National Council of Technological and Scientific Development, CNPq, Brazil (JGVM: Grant number 307828/2018-2; HS: Grant numbers 431990/2018-2 and 313423/2019-9; RFSA: Grant numbers 422561/2018-5 and 304257/2019-2). The funders had no role in study design, data collection and analysis, decision to publish, or preparation of the manuscript.

CRediT authorship contribution statement

Conceptualization, RFSA, JGVM, ESS; Study design and methodology: RFSA, JGVM, ESS, MGT, MLB; Provided data: MGT, MCNC, LMS, LLC, MLVA; Implemented the study and carried statistical analyses: ESS, RFSA; Discussed and interpreted the analyses: ESS, RFSA, JGVM, HS, MLVA; First draft of the manuscript: ESS, RFSA, JGVM, HS. All authors read and contributed with the manuscript. All authors reviewed the final manuscript and agreed to the published version of the manuscript.

Declaration of competing interest

The authors declare that they have no known competing financial interests or personal relationships that could have appeared to influence the work reported in this paper.

Data availability

Data will be made available on request.

Appendix A. Supplementary data

Supplementary data to this article can be found online at https://doi.org/10.1016/j.chaos.2023.113134.

References

[1] Paixão ES, Teixeira MG, Rodrigues LC. Zika, chikungunya and dengue: the causes and threats of new and reemerging arboviral diseases. BMJ Glob Health 2018;3. https://doi.org/10.1136/bmjgh-2017-000530.

[2] De Souza LJ. Dengue, Zika e Chikungunya – Diagnóstico, Tratamento e Prevenção. Editora Rubio; 2016.

[3] Galán-Huerta KA. The Zika virus disease: an overview. Med Univ 2016;18(71): 115–24. https://doi.org/10.1016/j.rmu.2016.05.003.

[4] Krauer F. In: Zika virus infection as a cause of congenital brain Abnormalities and Guillain – barre syndrome : systematic review; 2017. p. 1–27. https://doi.org/10.1371/journal.pmed.1002203.

[5] Luz KG, dos Santos GIV, de Vieira R, M.. Febre pelo vírus zika. Epidemiol Serv Saúde 2015;24(4):785–8. https://doi.org/10.5123/s1679-49742015000400021.

[6] Pialoux G, et al. Chikungunya, an epidemic arbovirosis. Lancet Infect Dis 2007;7 (5):319–27. https://doi.org/10.1016/S1473-3099(07)70107-X.

[7] Vu DM, Jungkind D, LaBeaud AD. Chikungunya virus. Clin Lab Med 2017;37(2): 371–82. https://doi.org/10.1016/j.cll.2017.01.008. Elsevier Inc.

[8] Balcan D, et al. Modeling the spatial spread of infectious diseases: the global epidemic and mobility computational model. J Comput Sci 2010;1(3):132–45. https://doi.org/10.1016/j.jocs.2010.07.002.

[9] Farnese C, et al. Analysis and control of epidemics. IEEE Control Syst Mag 2012;1: 19–21.

[10] Madar N, et al. Immunization and epidemic dynamics in complex networks. Eur Phys J B 2004;38(2):269–76. https://doi.org/10.1140/epjb/e2004-00119-8.

[11] Newman MEJ. The structure and function of complex networks. SIAM Rev 2003;45 (2):167–256. https://doi.org/10.1137/S003614450342480.

[12] Pastor-Satorras R, et al. Epidemic processes in complex networks. Rev Mod Phys 2015;87(3):925–79. https://doi.org/10.1103/RevModPhys.87.925.

[13] Stehlé J, et al. Simulation of an SEIR infectious disease model on the dynamic contact network of conference attendees. BMC Med 2011;9:1–15. https://doi.org/10.1186/1741-7015-9-87.

[14] Malik HAM, et al. Nature of complex network of dengue epidemic as a scale-free network. Healthc Inf Res 2019;25(3):182. https://doi.org/10.4258/hir.2019.25.3.182.

[15] Hendron RWS, Bonsall MB. The interplay of vaccination and vector control on small dengue networks. J Theor Biol 2016;407:349–61. https://doi.org/10.1016/j.jtbi.2016.07.034. Elsevier.

[16] Malik HAM. Modeling of internal and external factors affecting a complex dengue network. Chaos Solitons Fractals 2021;144:110694. https://doi.org/10.1016/j.chaos.2021.110694. Elsevier Ltd.

[17] Saba H, et al. Spatio-temporal correlation networks of dengue in the state of Bahia. BMC Public Health 2014;14:4–9. https://doi.org/10.1186/1471-2458-14-1085.

[18] Saba H, et al. Relevance of transportation to correlations among criticality, physical means of propagation, and distribution of dengue fever cases in the state of Bahia. Sci Total Environ 2018;618:971–6. https://doi.org/10.1016/j.scitotenv.2017.09.047. Elsevier B.V.

[19] Li L, et al. Analysis of transmission dynamics for zika virus on networks. Appl Math Comput 2019;347:566–77. https://doi.org/10.1016/j.amc.2018.11.042.

[20] Srivastav AK, et al. Spread of zika virus disease on complex network—a mathematical study. Math Comput Simul 2019;157:15–38. https://doi.org/10.1016/j.matcom.2018.09.014. Elsevier B.V.

[21] Rosário RS, et al. Motif-synchronization: a new method for analysis of dynamic brain networks with EEG. Physica A 2015;439:7–19. https://doi.org/10.1016/j.physa.2015.07.018.

[22] Araújo MLV, et al. Nonlocal dispersal of dengue in the state of Bahia. Sci Total Environ 2018;631–632:40–6. https://doi.org/10.1016/j.scitotenv.2018.02.198. Elsevier B.V.

[23] Donalisio MR, Freitas ARR, Von Zuben APB. Arboviruses emerging in Brazil: challenges for clinic and implications for public health. Rev Saude Publica 2017; 51:10–5. https://doi.org/10.1590/S1518-8787.2017051006889.

[24] Fantinato FFST, et al. Descrição dos primeiros casos de febre pelo vírus zika investigados em municípios da região nordeste do brasil, 2015. Epidemiol Serv Saude 2016;25(4):683–90. https://doi.org/10.5123/S1679-49742016000400002.

[25] Zanotto PMde A, Leite LCde C. The challenges imposed by Dengue, Zika, and Chikungunya to Brazil. Front Immunol 2018;9(August):1–6. https://doi.org/10.3389/fimmu.2018.01964.

[26] Flocchini P, Mans B, Santoro N. Exploration of periodically varying graphs. Lect Notes Comput Sci 2009;5878 LNCS:534–43. https://doi.org/10.1007/978-3-642-10631-6_55.

[27] Casteigts A, et al. Time-varying graphs and dynamic networks. Int J Parallel Emergent Distrib Syst 2012;5:387–408. https://doi.org/10.1007/978-3-642-22450-8_27.

[28] Nicosia V, et al. Components in time-varying graphs. Chaos 2012;22(2):023101. https://doi.org/10.1063/1.3697996.

[29] Tang J, et al. Small-world behavior in time-varying graphs. Phys Rev E Stat Nonlinear Soft Matter Phys 2010;81(5):81–4. https://doi.org/10.1103/PhysRevE.81.055101.

[30] Stefano Filho CA, Attux R, Castellano G. Can graph metrics be used for EEG-BCIs based on hand motor imagery? Biomed Signal Process Control 2018;40:359–65. https://doi.org/10.1016/j.bspc.2017.09.026. Elsevier Ltd.

[31] Prabodanie RAR, Stone L, Schreider S. Spatiotemporal patterns of dengue outbreaks in Sri Lanka. Infect Dis 2020;52(5):350–60. https://doi.org/10.1080/23744235.2020.1725108. Taylor & Francis.

[32] Saba H, et al. Synchronized spread of COVID-19 in the cities of Bahia, Brazil. Epidemics 2022;39(June 2021):100587. https://doi.org/10.1016/j.epidem.2022.100587. Elsevier B.V.

[33] Christina U, Matassa MS, Mimler M. TRANSVIEW : a program for matching universal transverse mercator (UTM) and geographic coordinates25; 1999.

[34] IBGE. MANUAIS TÉCNICOS EM GEOCIÊNCIAS - Acesso e Uso de Dados Geoespaciais n. 14, Ibge. Available at: https://loja.ibge.gov.br/manual-tecnico-em-geociencias-acesso-e-uso-de-dados-geoespaciais.html; 2019.

[35] Stott PH. The UTM grid reference system. J Soc Ind Archeology 1977;3(1):1–14.

[36] Brasil. Ministério da Saúde. Departamento de Informática do SUS. Transferência de Arquivos [Internet] [cited 2022 Jul 13] Available from: https://datasus.saude.gov.br/transferencia-de-arquivos/; 2022.

[37] IBGE. Instituto brasileiro de geografia e estatística (IBGE). Território e ambiente. Available at: https://cidades.ibge.gov.br/brasil/ba/panorama. [Accessed 9 May 2022].

[38] Filho ASN, et al. A spatio-temporal analysis of dengue spread in a Brazilian dry climate region. Sci Rep 2021;11(1):1–8. https://doi.org/10.1038/s41598-021-91306-z. Nature Publishing Group UK.

[39] Chan M, Johansson MA. The incubation periods of dengue viruses. PLoS ONE 2012; 7(11):1–7. https://doi.org/10.1371/journal.pone.0050972.

[40] World Health Organization. Dengue guidelines for diagnosis, treatment, prevention and control : new edition, Psychiatric News. World Health Organization.; 2009.

[41] Krow-Lucal ER, Biggerstaff BJ, Staples JE. Estimated incubation period for zika virus disease. Emerg Infect Dis 2017;23(5):841–4. https://doi.org/10.3201/eid2305.161715.

[42] da Vasconcelos PF, C.. Doença pelo vírus zika: um novo problema emergente nas Américas? Rev Pan-Amazônica Saúde 2015;6(2):9–10. https://doi.org/10.5123/s2176-62232015000200001.

[43] Zanluca C, et al. First report of autochthonous transmission of zika virus in Brazil. Mem Inst Oswaldo Cruz 2015;110(4):569–72. https://doi.org/10.1590/0074-02760150192.

[44] Barreto FR. Spread pattern of the first dengue epidemic in the city of Salvador, Brazil. BMC Public Health 2008;8:1–20. https://doi.org/10.1186/1471-2458-8-51.

[45] Dalvi APR, Braga JU. Spatial diffusion of the 2015–2016 zika, dengue and chikungunya epidemics in Rio de Janeiro municipality, Brazil. Epidemiol Infect 2019;147. https://doi.org/10.1017/S0950268819001250.

[46] Morato DG, et al. The spatiotemporal trajectory of a dengue epidemic in a medium-sized city. Mem Inst Oswaldo Cruz 2015;110(4):528–33. https://doi.org/10.1590/0074-0276140388.

[47] Santana LS, Braga JU. Spatial diffusion of zika fever epidemics in the municipality Salvador-Bahia, Brazil, in 2015-2016: Does Zika fever have the same spread pattern as Dengue and Chikungunya fever epidemics? Rev Soc Bras Med Trop 2020;53(December 2019):1–11. https://doi.org/10.1590/0037-8682-0563-2019.

[48] Skalinski LM, et al. The triple epidemics of arboviruses in Feira de Santana, brazilian northeast: epidemiological characteristics and diffusion patterns. Epidemics 2022;38. https://doi.org/10.1016/j.epidem.2022.100541.

[49] Li X, Ouyang G. Estimating coupling direction between neuronal populations with permutation conditional mutual information. NeuroImage 2010;52(2):497–507. https://doi.org/10.1016/j.neuroimage.2010.05.003. Elsevier Inc.

[50] Localidades | IBGE. Instituto brasileiro de geografia e estatística (IBGE). 2010. Available at: https://www.ibge.gov.br/geociencias/organizacao-do-territorio/estrutura-territorial/27385-localidades.html?=&t=acesso-ao-produto [Accessed May 26, 2022].